# Supplementary Appendix

This appendix has been provided by the authors to give readers additional information about their work.

Supplement to: Aksentijevich I, Masters SL, Ferguson PJ, et al. An autoinflammatory disease with deficiency of the interleukin-1–receptor antagonist. N Engl J Med 2009;360:2426-37.

# Supplementary Appendix:

## SUPPLEMENTARY METHODS

### Quantitative PCR

RNA was prepared from peripheral blood collected in PAXgene tubes (Qiagen) and converted to cDNA using Superscript II (Invitrogen). Quantitative polymerase chain reaction (q-PCR) was performed using TaqMan probes for *IL1RN* (Hs00277299_m1, Applied Biosystems) compared with 18S endogenous control.

### Protein Analysis

Washed whole blood was stimulated with 1ug/ml Ultrapure LPS E. coli K12 (Invivogen) for three hours and supernatants were collected. Western blotting was performed and probed using goat anti-IL-1Ra (Santa Cruz Biotechnology, sc-8479). To obtain white blood cells (WBC), red blood cells were lysed with ACK lysing solution (Quality Biologicals).

### Leukocyte Stimulation Assay

Leukocytes were washed and cultured at $2x10^6$ per ml in RPMI for 18 hours with or without 50ng/ml rhIL-1β (Peprotech); supernatants were collected and cytokine concentrations were measured using the Bio-Plex system (Bio-Rad). Unpaired T-tests were used to compare group data.

### Expression and Function of IL-1Ra Mutants

293T cells (ATCC) were transfected with an IL-1Ra construct (Origene) or mutants thereof using Fugene 6 (Roche). Cells were lysed in RIPA buffer with protease inhibitors (Roche). Functional analysis of supernatants was performed using the IL-1 responsive T-cell line D10.G4.1 (15).

### Immunohistochemistry

Skin biopsy tissue was obtained for diagnostic purposes. Sections of fixed paraffin embedded tissue were stained using anti - IL-17 antibody (R&D systems, AF-317-N).

### Intracellular cytokine assay

Peripheral blood mononuclear cells (PBMCs) were isolated by Ficoll centrifugation. Stimulation was performed on fresh or frozen PBMCs resuspended at 106 cells/ml in RPMI with 10% heat inactivated fetal calf serum (R10) with 1µg/mL anti-CD28 and anti-CD49d antibodies, with the addition of 1µg/mL *Staphylococcus* enterotoxin B (Sigma-Aldrich) or 5ng/mL phorbol myristyl acetate and 1µM ionomycin (Sigma-Aldrich). Cell cultures were propagated at 37°C for 16 hours in the presence of 1µg/mL brefeldin A (Sigma-Aldrich). Aqua Blue dead cell dye (Invitrogen) was added, and all cells were surface stained for CD3, CD4,

CD8, CD27, CD45RO, and stained after fixation/permeabilization for IL17, IFNγ, TNFα, and IL2. Cells were gated for live CD3+CD4+CD8- cells, and memory cells were selected as CD27+CD45RO+ and CD27-CD45RO+/-.

Flow cytometric analysis was performed using a LSR II (BD Biosciences, San Jose, CA). Allophycocyanin (APC), fluorescein isothiocyanate (FITC), phycoerythrin (PE), Cy7PE, Cy5.5PE, Cy5PE, Cy7APC, Texas Red PE, and Pacific Blue were used as the fluorophores. Analysis was made on a minumum of 300,000 cells using FlowJo software (TreeStar). Functional capacity was determined after Boolean gating, and further analysis was performed using Simplified Presentation of Incredibly Complex Evaluations (SPICE, version 4.1.6; Mario Roederer, Vaccine Research Center (VRC), National Institute of Allergy and Infectious Diseases [NIAID], NIH). All values used were background-subtracted. The percentage of memory CD4 T cells from patients, siblings, and parents expressing IL-17, IFNγ, TNF, and IL-2 was calculated.

SUPPLEMENTARY FIGURES

**Supplementary Figure 1. Radiographic, histological and MRI features of DIRA**

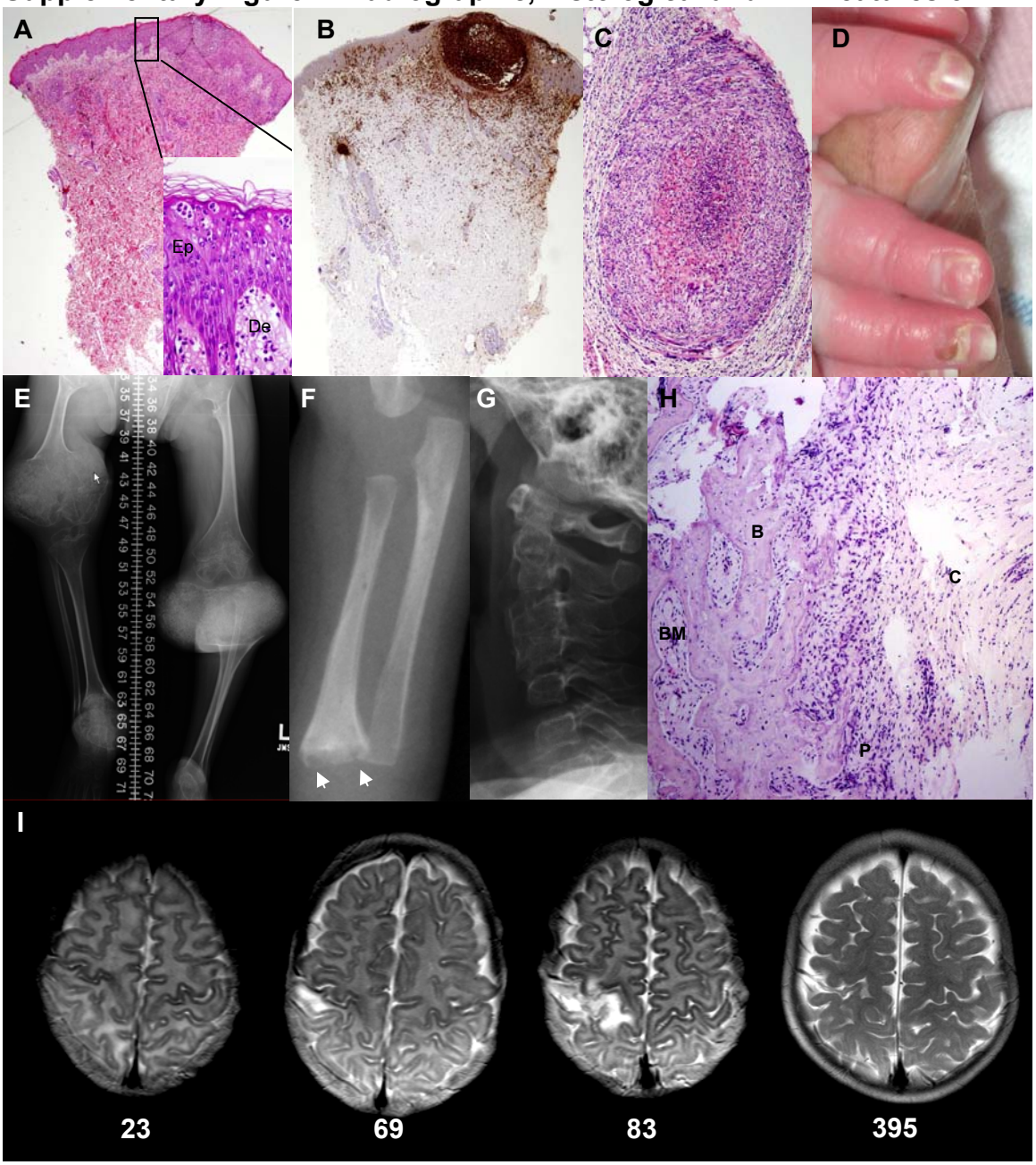


**Panels A and B** depict images from a skin biopsy. In Panel A a hematoxylin and eosin stain was performed (insert: epidermis (Ep), dermis (D)) and in Panel B myeloperoxidase staining indicates extensive neutrophilic infiltration (in brown) with a pustule around the hair shaft.

**Panel C** Connective tissue adjacent to a bone biopsy showed vasculitis in 2 vessels (only one vessel shown) with extensive neutrophilic infiltration and destruction of the vessel wall.

**Panel D** Nail changes similar to psoriasis with onychomadesis (separation of nail and nail bed) were seen in two patients.

**Panel E** shows an x-ray of Puerto Rican patient (#9) with epiphyseal ballooning affecting the distal and proximal epiphyses of several long bones.

**Panel F** Distal radial osteolytic lesions are marked by 2 white arrows.

**Panel G** shows partial fusion of the posterior elements of C2-C4 following osteolytic vertebral lesions.

**Panel H** shows bone biopsy with adjacent connective tissue (CT). Extensive bone (B) destruction is seen with extensive fibrosis of the bone marrow (BM).

**Panel I** depicts serially obtained T2 weighted axial MR images. On day 23 the MRI is normal, on day 69 there is edema in the right post central gyrus, and on day 83, this has progressed anteriorly into the precentral gyrus. On day 395, frank encephalomalacia of the postcentral gyrus is seen.

**Supplementary Figure 2. IL-1 receptor antagonist (IL-1Ra)**

**A**

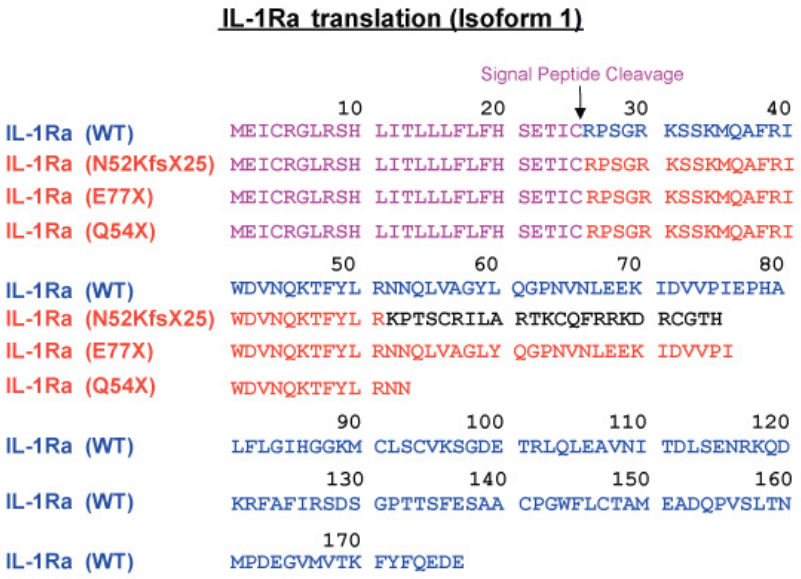


**B**

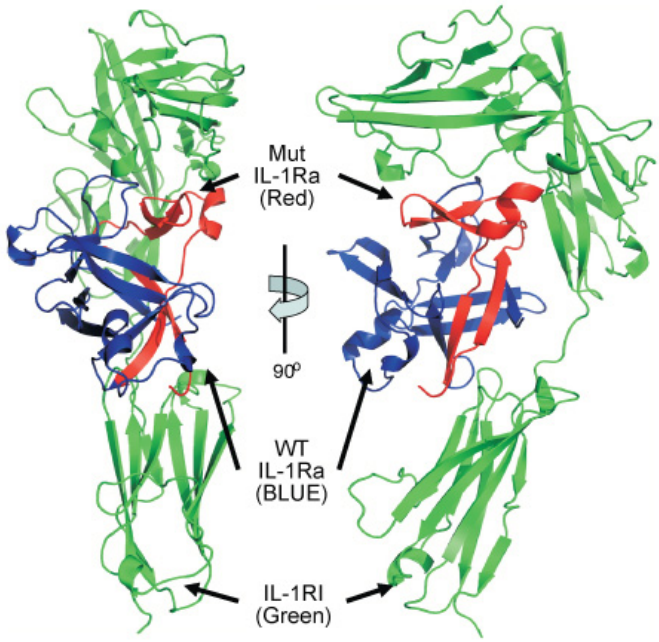


**C**

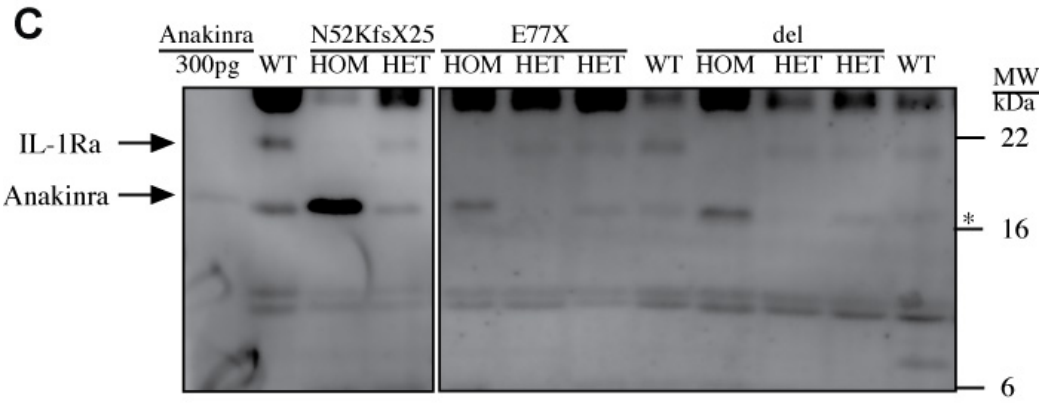

**Panel A** describes how DIRA mutations result in premature truncation of the IL-1Ra amino acid sequence. The frameshift mutation also introduces 24 missense amino acids into the protein (black). Residues 1–25 represent a signal peptide that is cleaved when secreted from the cell (violet).

**Panel B** Two views of the crystal structure of IL-1RI (green) in complex with IL-1Ra highlight the effects of the DIRA mutations on the modeled interaction between mutant IL-1Ra and the IL-1 receptor. Red shows the portion of the IL-1Ra protein present in the E77X truncation, and blue shows the remainder of the wildtype protein that is absent in all the truncated forms.

**Panel C** A larger image of the Western blot shown in Fig. 3 panel B. This image shows that truncated (lower molecular weight) IL-Ra proteins are absent in the homozygous patients as well as heterozygous carriers with the N52KfsX25 and E77X mutations. A band corresponding to the size of anakinra can also be observed in the patients undergoing treatment, slightly above a nonspecific band indicated by an asterisk.

## Supplementary Figure 3. TH17 and IFNγ producing cells in DIRA patients, their siblings and family controls

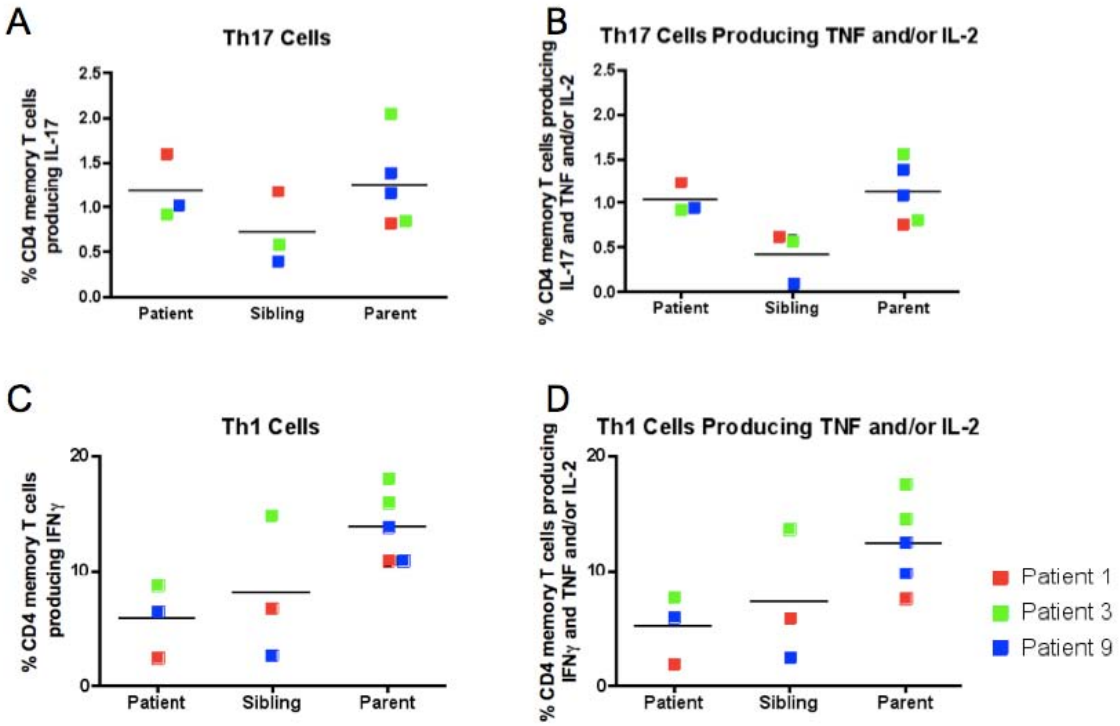


Cytokine production by memory CD4+ T cells after PBMCs were stimulated overnight with *Staphylococcus* enterotoxin B. The frequency of Th17 cells are depicted as percent of CD4+memory T cells. The production of TNF and IL-2 by the Th1 and Th17 cells was investigated
**Panel A** Frequency of CD4+ memory T cells that produce IL-17.
**Panel B** Frequency of CD4+ memory cells that produce IL-17 (Th17 cells) but also TNF and/or IL-2.
**Panel C** Frequency of CD4+ memory T cells that produce IFNγ.
**Panel D** Frequency of CD4+memory cells that produce IFNγ (Th1 cells) but also TNF and/or IL-2.

TNF is pro-inflammatory and is elevated in a number of autoimmune diseases, e.g. rheumatoid arthritis. IL-2 promotes the proliferation of CD4+ and CD8+ T cells and can thus amplify the an immune response. It may also be involved in the programming of CD8+ T cells for memory capacity and effector function. Studies of multifunctional Th1 cells show that they produce significantly more IFNγ per cell than monofunctional Th1 cells, so the total magnitude of response may be greater (1).

**Reference List**

(1) Seder RA, Darrah PA, Roederer M. T-cell quality in memory and protection: implications for vaccine design. Nat Rev Immunol 2008; 8(4):247-258.

## SUPPLEMENTARY TABLE

### Supplementary Table 1. Cytokines assayed post stimulation with human recombinant IL-1 β

| Group I Cytokines | Group II Cytokines |
|---|---|
| IL-1b | IFN-a2 |
| IL-1ra | IL-1a |
| IL-2 | IL-2ra |
| IL-4 | IL-3 |
| IL-5 | IL-12p40 |
| IL-6 | IL-16 |
| IL-7 | IL-18 |
| IL-8 | CTACK |
| IL-9 | GRO-a |
| IL-10 | HGF |
| IL-12(p70) | ICAM-1 |
| IL-13 | LIF |
| IL-15 | MCP-3 |
| IL-17 | M-CSF |
| Eotaxin | MIF |
| FGF basic | MIG |
| G-CSF | B-NGF |
| GM-CSF | SCF |
| IFN-g | SCGF-B |
| IP-10 | SDF-1a |
| MCP-1(MCAF) | TNF-B |
| MIP-1a | TRAIL |
| MIP-1b | VCAM-1 |
| PDGF bb | |
| RANTES | |
| TNF-a | |
| VEGF | |